Published in final edited form as:
Hear Res. 2010 May ; 263(0): 183–190. doi:10.1016/j.heares.2009.10.013.

Tympanic-membrane and malleus–incus-complex co-adaptations for high-frequency hearing in mammals

Sunil Puria[a,b,c,*] and **Charles Steele**[a]

[a]Department of Mechanical Engineering, 496 Lomita Mall, Stanford, CA 94305, USA

[b]Department of Otolaryngology – Head and Neck Surgery, Stanford CA 94305, USA

[c]Palo Alto Veterans Administration, Palo Alto, CA 94304, USA

Abstract

The development of the unique capacity for high-frequency hearing in many mammals was due in part to changes in the middle ear, such as the evolution of three distinct middle-ear bones and distinct radial and circumferential collagen fiber layers in the eardrum. Ossicular moment(s) of inertia (MOI) and principal rotational axes, as well as eardrum surface areas, were calculated from micro-CT-based 3-D reconstructions of human, cat, chinchilla, and guinea pig temporal bones. For guinea pig and chinchilla, the fused malleus–incus complex rotates about an anterior–posterior axis, due to the relatively lightweight ossicles and bilateral symmetry of the eardrum. For human and cat, however, the MOI calculated for the unfused malleus are 5–6 times smaller for rotations about an inferior–superior axis than for rotations about the other two orthogonal axes. It is argued that these preferred motions, along with the presence of a mobile malleus–incus joint and asymmetric eardrum, enable efficient high-frequency sound transmission in spite of the relatively large ossicular masses of these species. This work argues that the upper-frequency hearing limit of a given mammalian species can in part be understood in terms of morphological co-adaptations of the eardrum and ossicular chain.

Keywords

Middle ear; Malleus–incus complex; Ossicles; Tympanic membrane; Moment of inertia; Rotational motion; High-frequency hearing; Co-adaptation; Micro-CT

1. Introduction

Mammals are unique among vertebrates in their ability to hear high-frequency sounds. While reptiles, amphibians, and most fish do not hear above 5–7 kHz (Heffner and Heffner, 1998), and birds do not hear above 8–12 kHz (Dooling et al., 2000), mammals have upper-frequency limits of hearing that range from 10 kHz (for the elephant) to 90 kHz (for the wild mouse), and even higher for some species that use echolocation (Heffner and Heffner, 2008).

[*]Corresponding author. Address: 496 Lomita Mall, Durand Building, Stanford, CA, 94305, USA. Tel.: +1 650 723 8089; fax: +1 650 723 1778. puria@stanford.edu (S. Puria).

It is well established that the capacity for high-frequency hearing in mammals provides an important means for localizing sound. While studying the auditory cortex, Masterton et al. (1969) observed that there was an inverse correlation between the head size of an animal and it's upper-frequency limit of hearing, and concluded that head size was related to sound-localization ability (Masterton et al., 1969; Heffner and Heffner, 2008). There are three primary types of sound-localization cues: (1) Inter-aural time difference (ITD) cues, which are dominant primarily at low frequencies (typically below 500 Hz), and allow horizontal-plane localization; (2) Inter-aural level difference (ILD) cues, or spectral difference cues (e.g. due to "head shadow"), which are dominant at higher frequencies, and also enable horizontal-plane localization; and (3) Pinna-diffraction cues, which assist in vertical-plane localization and become important for frequencies above about 5 kHz in human (Shaw, 1966), and above about 8 kHz in cat (Musicant et al., 1990; Young et al., 1996). As the frequency increases, the wavelength becomes shorter, so in order to maintain the ILD cues for smaller heads it becomes necessary to hear higher frequencies. Thus, for both horizontal and vertical-plane localization, the ability to hear beyond 5–10 kHz becomes important – especially for animals with smaller head sizes.

Of the various physical characteristics that distinguish mammals from other vertebrates, several pertain to the biomechanics of hearing. For example, the presence of three distinct middle-ear bones is one of the criteria used for classifying fossilized or living animals as mammals (Masterton et al., 1969; Colbert and Morales, 1991); the presence of distinct radial and circumferential collagen fiber layers of the tympanic membrane (Lim, 1968; Funnell and Laszlo, 1982; Rabbitt and Holmes, 1986; Fay et al., 2006) is also unique to mammals; as are the elongation of the basilar membrane (Manley, 1971) and motility of the organ of Corti outer hair cells, which are responsible for the high sensitivity of the mammalian cochlea (Brownell et al., 1985). These adaptations, in addition to others, serve to endow mammals with their unique capacity for high-frequency hearing. While the mechanics of the cochlea and outer hair cells is being studied in a significant number of laboratories, less attention has been paid to the role of the middle-ear structures in mammalian high-frequency hearing, and this is the primary subject of the present work.

It has been known for some time that there is tremendous variability in the size and shape of the middle-ear ossicles across different mammalian species (Doran, 1879; Hemila et al., 1995; Nummela, 1995; Schmelzle et al., 2005), and that the morphometry of the eardrum also varies across species (Funnell and Laszlo, 1982). The mass of the malleus–incus complex is often thought to limit the upper-frequency of hearing (Hemila et al., 1995), but in practice this appears not to be the case (Ruggero and Temchin, 2002). We propose that in small mammals (e.g. guinea pig and chinchilla), with lighter and fused malleus–incus complexes, the prevalent motion of these bones across all frequencies is the classical "hinging" motion about the anterior–posterior axis, as can be inferred from motion measurements on guinea pig ossicles (Manley and Johnstone, 1974). However, in larger mammals (e.g. human and cat), with heavier malleus and incus bones but a flexible malleus–incus joint, we argue that a new "twisting" mode along the inferior–superior axis of the malleus may reduce the effective inertia and thus allow the middle ear to transmit sound at higher frequencies than would be possible otherwise. An asymmetry in the anterior and posterior eardrum areas, which is seen in human and cat but not in guinea pig and chinchilla,

is hypothesized to allow pressure in the ear canal to induce such a twisting motion of the malleus. Thus, for a given mammal, anatomical co-adaptations of the tympanic membrane and malleus–incus complex appear to be determining factors of the upper-frequency limit of the middle ear. Preliminary aspects of this work were previously presented (Puria et al., 2007, 2006).

2. Materials and methods

2.1. Temporal bone preparation

Cadaveric temporal bones from human, cat, chinchilla, and guinea pig were used for the reported morphometry measurements. To facilitate micro-CT scanning, each temporal bone was dissected to fit into as small a bore size as possible while keeping all structures of interest intact. Depending on the specimen, the bore diameter ranged from 20.5 to 39 mm. To prevent the tissue from drying out, each temporal bone was wrapped in cellophane before being placed inside the scanner bore. The human temporal bones were obtained from the Palo Alto VA Hospital, the cat temporal bone came from the Carolina Biological Supply Company (www.carolina.com), the guinea pig temporal bone came from the laboratory of Nik Blevins (MD) at Stanford University, and the chinchilla temporal bone was shipped frozen from Northwestern University by Mario Ruggero (PhD).

2.2. Micro-CT imaging

The vivaCT 40 micro-CT scanner (SCANCO Medical AG; www.scanco.ch), located at the Palo Alto VA Hospital, was used for this study. The scanning parameters and procedures, as well as segmentation and volume reconstruction methods, have been described in two previous publications (Sim et al., 2007; Sim and Puria, 2008).

2.3. Determining ossicular moments of inertia (MOI)

It was possible to produce segmentations of the ossicles from the scanned images using automatic contouring techniques, since the density of the bone was sufficiently high compared to that of the surrounding air and soft tissue (Sim et al., 2007). Stacks of segmented slices were then combined to construct the 3-D volumes of each ossicle. These 3-D volumes were then used to calculate the centers of mass and moments of inertia (MOI) for the malleus, incus, and the combined malleus and incus. For the present study, each bone was assumed to have a uniform density, though in the future more accurate results might be obtained by taking into account the different density of the vascular regions within each bone.

An “inertia matrix” was initially calculated for each ossicle based on the scan reference frame. The inertia matrices were also recalculated using a coordinate system relative to the center of gravity of each given rigid body, such that all off-diagonal terms were zero simultaneously. The principal axes and corresponding three principal MOI were calculated from the eigenvectors and eigenvalues of the inertia matrix for each bone in the human and cat cases, and for the fused malleus–incus and stapes in the chinchilla and guinea pig cases. See (Sim et al., 2007) for calculation details. The MOI calculations were all normalized by density.

2.4. Determining eardrum surface areas

To determine the eardrum anterior and posterior surface areas, the 3-D eardrum shapes were reconstructed after performing manual segmentation of eardrum slices. The manubrium was segmented and registered in the same reference frame as the eardrum surface. The segmentation and reconstruction were performed using the vivaCT 40 scanner software, and the resulting data were exported in STL (Standard Tessellation Language) format and then imported into another program called RapidForm (INUS Technology). The axis along the length of the manubrium was used to divide the eardrum into anterior and posterior sides, and Rapid- Form was used to calculate the eardrum surface area between the manubrium and the tympanic annulus for each side.

3. Results

3.1. Principal moments of inertia

At frequencies below a few kHz, middle-ear dynamics are limited by the suspensory ligaments and tendon attachments of the ossicles to the surrounding bony walls, which behave approximately as springs with stiffnesses that decrease as frequency increases (Sim and Puria, 2008). At high frequencies, the rotational and translational inertias of the ossicles are thought to be the limiting factors affecting the transmission of sound from the eardrum to the cochlea. A cross-species comparison of ossicular rotational inertias is presented here, to provide a basis for examining the relationship between these inertias and the upper-frequency limit of hearing in each species.

The three-dimensional reconstructions of the guinea pig and chinchilla ossicles are shown in Fig. 1, and those of the human and cat ossicles are shown in Fig. 2. Orthogonal rotational axes, corresponding to the maximum (red), minimum (blue), and intermediate (green) rotational moment(s) of inertia (MOI), are shown passing through the centers of gravity of the stapes and fused malleus–incus complex in Fig. 1, and through the centers of gravity of the stapes and unfused malleus and incus in Fig. 2. For the fused malleus–incus complex of the chinchilla and guinea pig, the axes for the minimum MOI (blue solid lines in Fig. 1) lie along the anterior–posterior direction. The minimum MOI for the chinchilla is around 3–4 times smaller than the intermediate and maximum MOI, and for the guinea pig it is 1.7–2.3 times smaller.

The axis for the minimum MOI of the unfused human malleus lies along the superior–inferior direction, which is perpendicular to that of the minimum MOI for the chinchilla and guinea pig. The minimum MOI for human is around six times smaller than the intermediate and maximum MOI. For the incus, the minimum MOI is less than half that of the maximum MOI. These results are consistent with our previous reports in three other human temporal bone ears (Sim et al., 2007).

For the cat, the axis directions and relationships between the minimum MOI and the intermediate and maximum MOI are similar to those in the human bones, albeit with lower values overall due to the cat ossicles being smaller and lighter.

3.2. Malleus morphometry

The MOI calculations suggest that at high frequencies, when ossicular motions become limited by inertial rather than stiffness considerations, the physiological responses for the human and cat ossicles may differ from those of the chinchilla and guinea pig. The most striking difference between these predicted high-frequency motions (indicated by black double arrows in Figs. 1 and 2) is the possibility of a “twisting” motion about the superior–inferior axis of the malleus for both human and cat, as opposed to the classical “hinging” motion about the anterior–posterior axis of the fused malleus–incus complex for the chinchilla and gerbil. If these predictions are correct, then the structure of the malleus in each species should be such that it can support the indicated motions. This is explored in Fig. 3, which compares micro-CT cross-sections of the malleus.

The cross section of the human malleus is circular in shape and is, with the exception of blood vessels, solid. The cross section of the cat malleus is more elliptical, but appears to be filled with fluid, which makes it lighter in weight than if it were solid. Both of these shapes are well suited for the proposed twisting motion. On the other hand, the cross section of the guinea pig or chinchilla malleus is not circular, but appears to be shaped more like an I-beam with a thin bony member between a flatter lateral section and a somewhat circular medial rod. This type of shape would not support a twisting motion, but is well suited for the classical hinging motion.

3.3. Malleus–incus joint (MIJ)

From the scanned micro-CT images, it is possible to obtain a 3-D reconstruction of the malleus–incus joint (MIJ). As first reported by Helmholtz (1868), the MIJ is saddle-shaped. It is well established that the MIJ is a synovial joint filled with a high-viscosity fluid (Marquet, 1981). We have done extensive studies of the morphometry of the human MIJ, which indicate an average minimum gap between the malleus and incus of 40 μm, and a maximum gap of as much as 320 μm (Sim and Puria, 2008). The viscous gap between the two bones indicates that the joint is mobile. Similar preliminary observations have also been made for the cat MIJ.

Conversely, for the chinchilla and guinea pig there is no clear gap between the malleus and incus in the cross-sectional micro-CT images, and thus the bones are considered to be fused. These observations are consistent with previous reports in the literature regarding joint immobility in guinea pig and chinchilla (Vrettakos et al., 1988; Amin and Tucker, 2006).

3.4. Tympanic-membrane asymmetry

Based on the above predictions regarding the twisting motion of the human and cat malleus at high frequencies, the sound pressure in the ear canal would need to be able to initiate such a motion through the tympanic membrane. We hypothesize that one way for this to occur would be through an asymmetry in the tympanic- membrane surface areas on either side of the manubrium.

Three-dimensional reconstructions of the eardrum were obtained for all four species studied. A line drawn through the malleus handle, extended to the inferior edge of the tympanic

annulus, was used as the dividing line between the anterior and posterior sections of the tympanic membrane. In Fig. 4, these are grouped according to species with a mobile MIJ (top row) or fused MIJ (bottom row). Posterior areas (blue) are larger than the anterior areas (yellow) for human and cat, with mobile joints, while the two areas are approximately equal for the chinchilla and guinea pig, with fused joints.

Fig. 5 contains a plot of the calculated anterior, posterior, and total surface areas for all four species in increasing order of their upper-frequency limit of hearing. Posterior areas (blue) are larger in comparison to the anterior areas (yellow) by a factor of 1.6 for human and 1.8 for cat, with a mobile MIJ. On the other hand, the area ratio is approximately 1.0 for chinchilla and 1.1 for guinea pig, with a fused MIJ. The total eardrum areas are within 12% of previous reports, except in guinea pig where the micro-CT-based area was 34% higher than previous reports (Nummela, 1995). The asymmetric eardrum is consistent with the predicted high-frequency twisting motion of the malleus with a mobile MIJ, while the symmetric eardrum is consistent with the predicted high-frequency hinging motion with a fused MIJ.

4. Discussion

It is currently believed that the three-bone ossicular chain in the mammalian middle ear developed independently at about the same time as the single-ossicle system found in non-mammalian vertebrates (Manley, 2009, this issue). This was a divergence and not a result of progressive functional improvements as was previously thought. However, as a result, the mammalian middle ear was able to transmit high-frequency sounds better than the single-ossicle system. This could then be exploited by parallel changes in the inner ear and the evolving brain to lead to an increase in the upper-frequency limit of hearing, which, combined with a greater capacity for neural computations due to the more complex mammalian brain, could then have led to the ability to perform sound localization using high-frequency cues (Manley, 2009, this issue). Given this premise, we argue that the specific morphologies of the tympanic membrane and the three ossicles were then free to co-evolve so as to further optimize the transmission of sound between the ear canal and the cochlea.

In species for which data are available, including human and cat, there is good correspondence between the middle-ear pressure gain and the threshold of hearing (Dallos, 1973; Puria et al., 1997), which suggests that the high-frequency hearing sensitivity is limited by the middle ear. It is known that the size of the mammalian hearing structures increases with body size, and it has been suggested that the upper-frequency limit of hearing is inversely proportional to the cube root of the ossicular mass (Nummela, 1995). However, Hemila et al. (1995) have pointed out inconsistencies in using ossicular mass as a limiting factor, observing that behaviorally the upper-frequency limit of hearing for the cat is only about “15% smaller than that of the mouse, although the cat ossicles are 50 times heavier”. Differences in the total-eardrum-area- to-stapes-footplate-area ratio, malleus-to-incus lever ratio, and cochlear specific input impedance do not appear to explain this discrepancy (Puria and Steele, 2008).

How, then, might the middle ear achieve good sound transmission at both high and low frequencies in humans and other mammals? At low frequencies (typically below 3–4 kHz), middle-ear mechanics can be well characterized by a hinging motion through the center of gravity of the malleus–incus complex, as described by Békésy (1960), Wever and Lawrence (1954), and others (see Fig. 6A). At high frequencies, the malleus and incus motions are more complicated, and involve movement in all three dimensions (Decraemer et al., 1994; Decraemer and Khanna, 1995; Willi et al., 2002; Sim et al., 2003). However, these complicated motions remain difficult to interpret.

4.1. Rotational Inertia of the malleus–incus complex

We hypothesize that, for human and cat at high frequencies, the hinging motion of the malleus and incus is limited by a large associated moment of inertia (MOI), such that another type of rotational motion of the malleus, along an axis with a smaller MOI, effectively takes over. Rotational MOI for the ossicles were calculated based on micro-CT imaging data to test this idea, and the results show that the minimum MOI for the malleus is associated with the long axis of the malleus body (inferior–superior) in both human (see Fig. 6B) and cat, and the maximum MOI is that associated with the classical anterior–posterior hinging axis. As shown in Fig. 2, the ratio of the maximum to minimum MOI is about a factor of six in human and cat, which implies that the preferred motion of the malleus is twisting-like (Fig. 6B), and the classical hinging motion is not optimal from a rotational inertia standpoint (though at low frequencies it may be preferable due to stiffness considerations). But how might this twisting motion of the malleus be transferred to the incus?

A shift in rotational axis needs to occur in the joint between the malleus and incus in order for the twisting motion of the malleus to produce incus motion suitable for driving the stapes. It is hypothesized that the saddle-shaped malleus–incus joint accomplishes this by effectively acting like a pair of biological “gears” similar to the helical or bevel gears found in machinery (see Fig. 6C). Such “gears” would only be required in larger mammals, like humans and cats, where the MOI due to ossicle mass is relatively large. To test this hypothesis, 3-D rotational motions of the ossicles are needed. Willi et al. (2002) made two rotational velocity measurements and a translational motion measurement of the malleus and incus, which provide evidence that the human MIJ is mobile. However, the ratios of motion that they reported are difficult to interpret in terms of the present hypothesis.

There have been several published analog circuit models of the middle ear where the reported region of validity is higher than 5 kHz. In these models, it was observed that the malleus and incus masses for the corresponding circuit elements were at least 3–5 times lighter than their measured masses for human and cat (Rosowski and Merchant, 1995; Puria and Allen, 1998; Parent and Allen, 2007; O’Connor and Puria, 2008). The fact that one-dimensional circuit models tend to require much lower mass terms than those of the ossicles measured in isolation, in order to match physiological measurements at high frequencies (e.g. ossicular velocity, middle-ear impedance, and reflectance), is consistent with the idea that the actual physiological motions of the ossicles at high frequencies are primarily rotational rather than translational. The lower inertias corresponding to rotational motions,

as compared to the higher inertias for translational motions, could account for some of the disparity between modeled and measured mass terms. Previously, only rotations about the anterior–posterior axis were considered. In the present work a new rotation about the inferior–superior axis of the mallei of larger mammals is proposed, which may become important at frequencies above where the anterior–posterior axis inertia becomes too large.

A corollary of the gear hypothesis is that in smaller mammals, like guinea pigs and chinchillas, since the ossicular MOI for the classical hinging axis is already small, middle-ear "gears" would not be needed. This is consistent with the fact that these smaller mammals have fused malleus–incus joints (Vrettakos et al., 1988; Amin and Tucker, 2006). The proposed twisting motion of the malleus also manifests itself in the anatomical structure of the tympanic membrane.

4.2. Tympanic membrane morphometry and ultrastructure

The eardrum consists of a large "pars-tensa" section and a smaller "pars-flaccida" section. The pars-tensa section is composed of four main layers (Lim, 1968, 1970). The two middle layers, unique to mammals, consist of a layer of circumferentially-oriented collagen fibers and a layer of radially-oriented collagen fibers, and both layers contribute to the mechanical stiffness of the eardrum (Funnell and Laszlo, 1982; Rabbitt and Holmes, 1986; Fay et al., 2006, 2005). The other layers consist largely of relatively flexible epidermal and mucosal tissue that mostly contributes to the overall mass of the eardrum.

Figs. 4 and 5 show that, of the two animals studied with a mobile joint, there is asymmetry in the areas of the posterior and anterior pars-tensa regions. We hypothesize that such an asymmetry can produce a force differential on the two edges of the manubrium, such that a twisting motion of the malleus can result.

Initial estimates of the eardrum material properties suggest a difference in the effective Young's modulus, a measure of elasticity, between the anterior and the posterior sides of the eardrum (Fay et al., 2005). Differences in the ultrastructure of the anterior and posterior sides of the eardrum could also be a factor leading to twisting motion. This is not yet well established, but is currently being investigated using electron microscopy (Jackson et al., 2009, this issue).

5. Summary

5.1. Co-adaptation of the tympanic membrane and malleus–incus complex

The results of this work suggest that the mass and shape of the malleus and incus, the mobility of the malleus–incus joint (MIJ), the eardrum asymmetry as measured by the ratio of the posterior and anterior areas (A_{post}/A_{ant}), and the upper-frequency limit of hearing (Fay, 1988) are all interdependent. Table 1 shows a summary of these relationships. One caveat to keep in mind is that the morphometry calculations reported in Table 1 are for $N = 1$ for each of the three species, except for the human minimum moment- of-inertia (MOI) calculation, in which three other temporal bone ears (Sim et al., 2007) were averaged with the present ear. The relationships in Table 1 can perhaps best be appreciated through the following pair-wise species comparisons.

5.1.1. Human vs chinchilla—Humans have a malleus + incus (M + I) mass that is four times heavier than that of chinchilla, and yet have similar upper-frequency hearing limits of 20 and 23 kHz, respectively. An explanation for this is that their minimum MOI are similar. To make use of the low minimum MOI along the inferior–superior axis, humans co-adapted an asymmetric eardrum, a malleus with a circular cross section, and a mobile MIJ. Conversely, to make use of the minimum MOI along the anterior–posterior axis, it is more efficient for the chinchilla to have a symmetric eardrum about the malleus, a strong I-beam-like malleus, and no slippage due to the fused MIJ.

5.1.2. Chinchilla vs cat—Comparing the chinchilla to the cat, we see that they both have similar M + I masses. However, the chinchilla has an upper-frequency hearing limit of 23 kHz, while for the cat it is 64 kHz – nearly three times higher. Consistent with our proposition, this could be explained as being due to the cat malleus having a lower-inertia twisting mode at high frequencies, enabled by an asymmetric eardrum and flexible MIJ, while the chinchilla malleus–incus complex would exhibit a hinging mode with a higher minimum MOI at high frequencies, mediated by a symmetric eardrum.

5.1.3. Guinea pig vs cat—A similar story emerges if we look at guinea pig and cat, the two animals with the highest upper-frequency hearing limits of those studied here. Even though the cat has more than twice the M + I mass, it has a higher upper-frequency hearing capability than the guinea pig. The cat has a mobile MIJ and asymmetric eardrum, whereas the guinea pig has a fused MIJ and a symmetric eardrum. ever, the cat's minimum MOI is higher than the guinea pig's instead of being lower. This is one inconsistency in our argument, though a possible explanation is that in the present calculations we have not taken the lower density fluid region of the bone into account, as seen in the micro-CT scan cross section of the cat malleus (Fig. 3).

5.1.4. Chinchilla vs guinea pig—For chinchilla and guinea pig, the two animals with a fused malleus–incus joint, the ossicular mass is a determining factor for the upper-frequency hearing limit, since the other factors of malleus shape and eardrum symmetry are all similar.

The above pair-wise comparisons support the idea that specific co-adaptations of the tympanic membrane and malleus–incus complex morphologies, can in part explain the range of upper-frequency hearing limits across different mammalian species.

Acknowledgments

We thank Jae Hoon Sim and Minyong Shin for the help with the calculations and Kevin N. O'Connor for help with the manuscript. We also thank Professor Geoffrey A. Manley for providing feedback and comments on an earlier draft. This work was supported by Grant No. R01 DC 005969 from the NIDCD of the NIH.

References

Amin S, Tucker AS. Joint formation in the middle ear: lessons from the mouse and guinea pig. Dev Dyn. 2006; 235:1326–1333. [PubMed: 16425222]

Békésy, Gv. Experiments in Hearing. AIP Press; New York: 1960.

Brownell WE, Bader CR, Bertrand D, de Ribaupierre Y. Evoked mechanical responses of isolated cochlear outer hair cells. Science. 1985; 227:194–196. [PubMed: 3966153]

Colbert, EH.; Morales, M. Evolution of the Vertebrates: A History of the Backboned Animals Through Time. Wiley-Liss; New York: 1991.

Dallos, P. The Auditory Periphery; Biophysics and Physiology. Academic Press; New York: 1973.

Decraemer W, Khanna S. Malleus vibration modelled as rigid body motion. Acta Otorhinolaryngol Belg. 1995; 49:139–145. [PubMed: 7610906]

Decraemer WF, Khanna SM, Funnell WR. A method for determining three-dimensional vibration in the ear. Hear Res. 1994; 77:19–37. [PubMed: 7928731]

Dooling, RJ.; Lohr, B.; Dent, ML. Hearing in birds. In: Dooling, RJ.; Fay, RR.; Popper, AN., editors. Comparative Hearing: Birds and Reptiles. Springer; 2000. p. 308-359.

Doran AHG. Morphology of the mammalian ossicular auditus. Trans Linnean Soc 2nd Ser. 1879; 2:371–497.

Fay J, Puria S, Decraemer WF, Steele C. Three approaches for estimating the elastic modulus of the tympanic membrane. J Biomech. 2005; 38:1807–1815. [PubMed: 16023467]

Fay JP, Puria S, Steele CR. The discordant eardrum. Proc Natl Acad Sci USA. 2006; 103:19743–19748. [PubMed: 17170142]

Fay, RR. Hearing in Vertebrates: A Psychophysics Databook. Hill-Fay Associates; Winnetka, Ill: 1988.

Funnell WR, Laszlo CA. A critical review of experimental observations on ear-drum structure and function. ORL J Otorhinolaryngol Relat Spec. 1982; 44:181–205. [PubMed: 7050811]

Heffner, HE.; Heffner, RS. High-frequency hearing. Dallos, P.; Oertel, D., editors. Audition. Elsevier; San Diego: 2008. p. 55-60.

Heffner, RS.; Heffner, HE. Hearing. In: Greenberg, G.; Haraaway, MM., editors. Comparitive Psychology, A Handbook. Routledge: 1998. p. 290-3330.

Helmholtz, HLF. Die Mechanik der Gehorknochelchen und des Trommelfells. In: Buck, AH.; Smith, N., editors. Pflug Arch ges Physiol Menschen Tiere 1. 1868. p. 1-60.The mechanism of the ossicles of the ear and the membrana tympani, 1873

Hemila S, Nummela S, Reuter T. What middle ear parameters tell about impedance matching and high frequency hearing. Hear Res. 1995; 85:31–44. [PubMed: 7559177]

Jackson RP, Ricci T, Chlebicki C, Krasieva T, Zalpuria R, Triffo W, Puria S. Multiphoton and electron microscopy of collagen in ex vivo, human tympanic membrane. Guest Editor Sunil Puria in MEMRO 2009 issue of Hear Res. 2009

Lim DJ. Tympanic membrane. Electron microscopic observation I: pars tensa. Acta Otolaryngol. 1968; 66:181–198. [PubMed: 4974041]

Lim DJ. Human tympanic membrane. An ultrastructural observation. Acta Otolaryngol. 1970; 70:176–186. [PubMed: 5477148]

Manley GA. Some aspects of the evolution of hearing in vertebrates. Nature. 1971; 230:506–509. [PubMed: 4927749]

Manley GA. An evolutionary perspective on middle ears. Guest Editor Sunil Puria, in MEMRO 2009 issue of Hear. 2009; 263:3–8.

Manley GA, Johnstone BM. Middle-ear function in the guinea pig. J Acoust Soc Am. 1974; 56:571–576. [PubMed: 4414678]

Marquet J. The incudo-malleal joint. J Laryngol Otol. 1981; 95:543–565. [PubMed: 7252336]

Masterton B, Heffner H, Ravizza R. The evolution of human hearing. J Acoust Soc Am. 1969; 45:966–985. [PubMed: 5791616]

Musicant AD, Chan JC, Hind JE. Direction-dependent spectral properties of cat external ear: new data and cross-species comparisons. J Acoust Soc Am. 1990; 87:757–781. [PubMed: 2307774]

Nolk. Crossed Helical Gears. 2000. Available from: <http://www.ul.ie/~nolk/gears.htm#Gear%20types>

Nummela S. Scaling of the mammalian middle ear. Hear Res. 1995; 85:18–30. [PubMed: 7559173]

O'Connor KN, Puria S. Middle-ear circuit model parameters based on a population of human ears. J Acoust Soc Am. 2008; 123:197–211. [PubMed: 18177151]

Parent P, Allen JB. Wave model of the cat tympanic membrane. J Acoust Soc Am. 2007; 122:918–931. [PubMed: 17672641]

Puria S, Allen JB. Measurements and model of the cat middle ear: evidence of tympanic membrane acoustic delay. J Acoust Soc Am. 1998; 104:3463–3481. [PubMed: 9857506]

Puria S, Peake WT, Rosowski JJ. Sound-pressure measurements in the cochlear vestibule of human-cadaver ears. J Acoust Soc Am. 1997; 101:2754–2770. [PubMed: 9165730]

Puria, S.; Shin, M.; Sim, JH.; Tuck-Lee, J.; Steele, CR. MicroCT imaging of the middle ear and the inner ear-Invited talk. ARO Denver CO; 2007.

Puria, S.; Sim, JH.; Shin, M.; Tuck-Lee, J.; Steele, CR. Middle ear morphometry from cadaveric temporal bone microCT imaging. In: Eiber, A.; Huber, A., editors. Middle Ear Mechanics in Research and Otology. World Scientific; Zurich, SW: 2006.

Puria, S.; Steele, CR. Mechano–Acoustical Transformations. Dallos, P.; Oertel, D., editors. Academic Press; San Diego: 2008. p. 165-200.

Rabbitt RD, Holmes MH. A fibrous dynamic continuum model of the tympanic membrane. J Acoust Soc Am. 1986; 80:1716–1728. [PubMed: 3794078]

Rosowski JJ, Merchant SN. Mechanical and acoustic analysis of middle-ear reconstruction. Am J Otol. 1995; 16:486–497. [PubMed: 8588650]

Ruggero MA, Temchin AN. The roles of the external, middle, and inner ears in determining the bandwidth of hearing. Proc Natl Acad Sci USA. 2002; 99:13206–13210. [PubMed: 12239353]

Schmelzle T, Nummela S, Sanchez-Villagra MR. Phylogentic transformations of the ear ossicles in marsupial mammals, with special reference to diprotodontians: a character analysis. Ann Carnegie Museum. 2005; 74:189–200.

Shaw EA. Earcanal pressure generated by a free sound field. J Acoust Soc Am. 1966; 39:465–470. [PubMed: 5907617]

Sim JH, Puria S. Soft tissue morphometry of the malleus–incus complex from micro-CT imaging. J Assoc Res Otolaryngol. 2008; 9:5–21. [PubMed: 18311579]

Sim, JH.; Puria, S.; Steele, CR. Three-Dimensional measurements and analysis of the isolated malleus–incus complex. In: Gyo, K.; Wada, H.; Hato, N.; Koike, T., editors. Middle Ear Mechanics in Research and Otology. World Scientific; Matsuyama, Japan: 2003.

Sim JH, Steele CR, Puria S. Calculation of inertia properties of the malleus–incus complex using micro-CT imaging. J Mech Mater Struct. 2007; 2:1515–1524.

Vrettakos PA, Dear SP, Saunders JC. Middle ear structure in the chinchilla: a quantitative study. Am J Otolaryngol. 1988; 9:58–67. [PubMed: 3400821]

Wever, EG.; Lawrence, M. Physiological Acoustics. Princeton University Press; Princeton: 1954.

Willi UB, Ferrazzini MA, Huber AM. The incudo–malleolar joint and sound transmission losses. Hear Res. 2002; 174:32–44. [PubMed: 12433394]

Young ED, Rice JJ, Tong SC. Effects of pinna position on head-related transfer functions in the cat. J Acoust Soc Am. 1996; 99:3064–3076. [PubMed: 8642117]

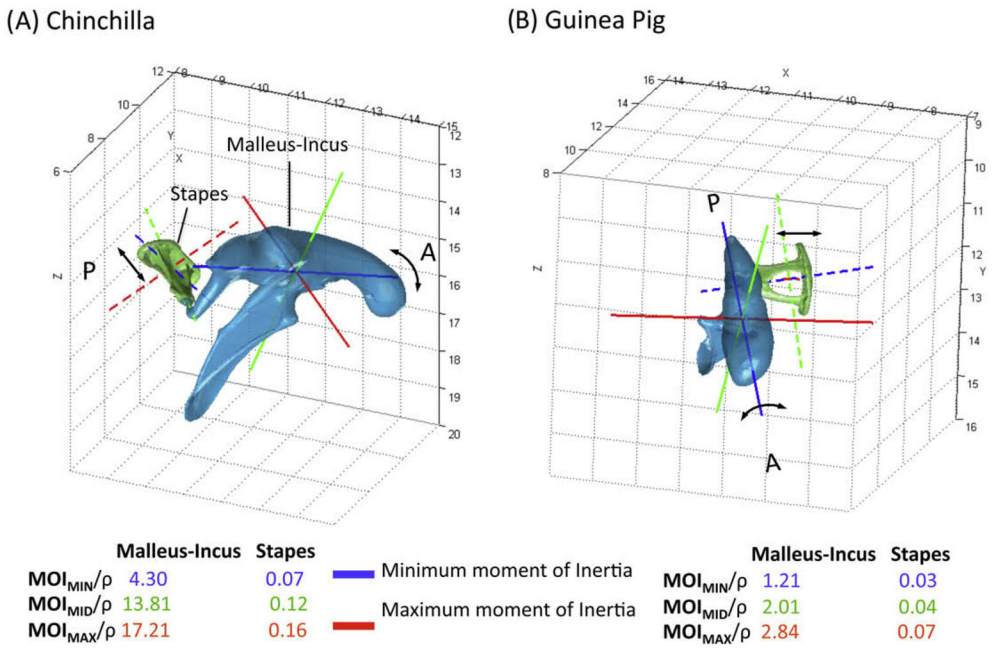

Fig. 1.

Moments of inertia (MOI) normalized by density (ρ) for the chinchilla (A) and guinea pig (B) ossicles. Because the malleus and incus bones in the chinchilla and guinea pig are fused, the MOI are calculated as though they were one bone (solid lines). Blue indicates axes associated with the minimum MOI, red the maximum MOI, and green the intermediate MOI. The dashed lines indicate the respective MOI for the stapes. The black arrows indicate the expected primary motions of the fused malleus–incus complex and stapes at high frequencies. The numbers along the edges of the coordinate axes are in mm. “P” and “A” indicate posterior and anterior sides, respectively.

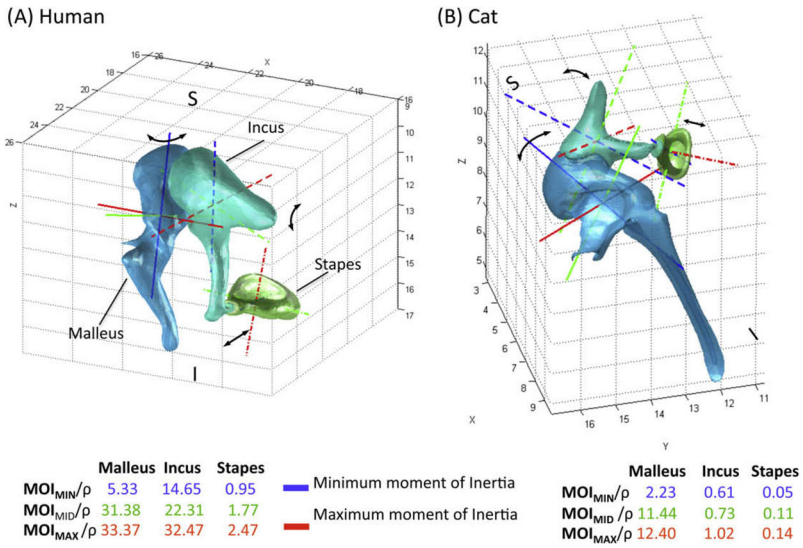

Fig. 2.

MOI normalized by density (ρ) for the human (A) and cat (B) ossicles. Because the malleus and incus bones in the human and cat are not fused, the MOI are calculated separately for each bone. Blue indicates axes associated with the minimum MOI, red the maximum MOI, and green the intermediate MOI. The black arrows indicate the predicted primary motions of the malleus, incus, and stapes at high frequencies. “S” and “I” indicate superior and inferior sides, respectively.

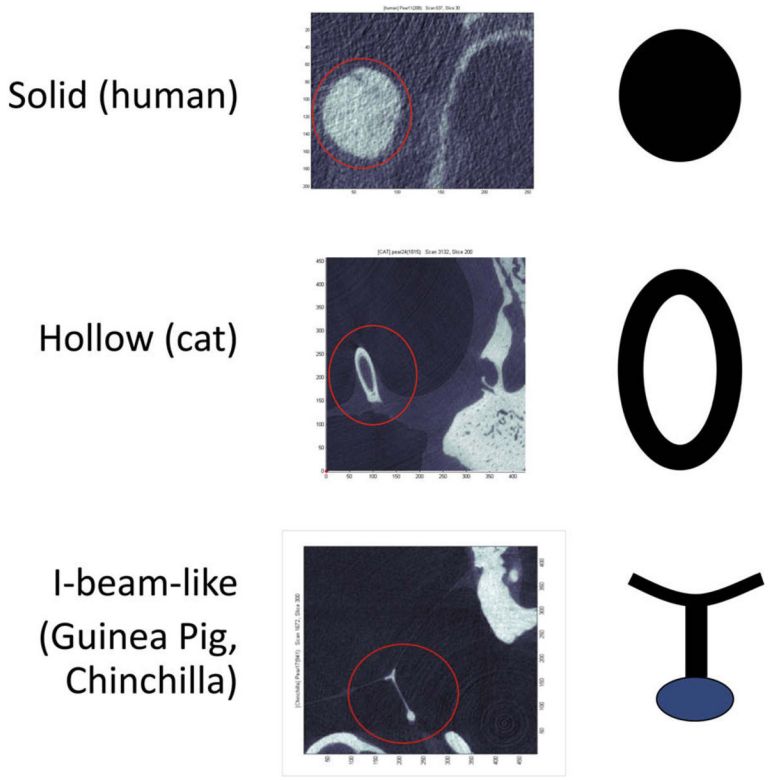

Fig. 3.

Cross species comparisons of malleus cross-sections. A round cross section (human and cat) could support “twisting” motion, while an I-beam-like cross section (guinea pig and chinchilla) would only support on-axis forces resulting from a “hinging” type of motion.

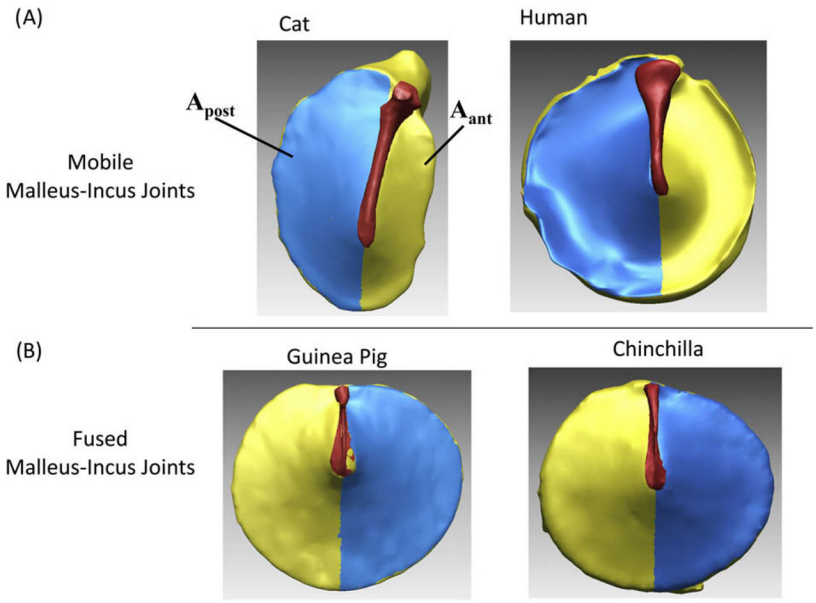

Fig. 4.

Tympanic membrane surface area asymmetry for human and cat, with a mobile malleus–incus joint (MIJ) (top row), and guinea pig and chinchilla, with a fused MIJ (bottom row). The manubrium of the malleus divides the membrane into posterior and anterior sections. Blue and yellow areas indicate the posterior area (A_{post}) and anterior area (A_{ant}) respectively.

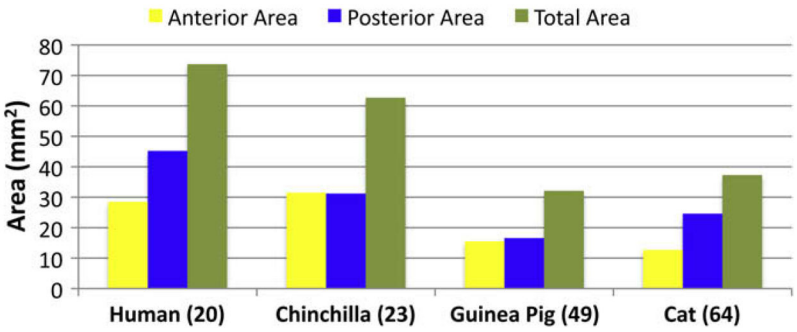

Fig. 5.

The calculated anterior, posterior, and total tympanic membrane areas for the four species studied, arranged in order of increasing upper-frequency limit of hearing (indicated in parentheses after the species name, in units of kHz). The posterior to anterior area ratios for human and cat, with mobile malleus–incus joints (MIJ), is approximately 1.6 and 1.9 respectively, while it is 1.0 and 1.1 for chinchilla and guinea pig respectively, with fused MIJ (N = 1 for each species).

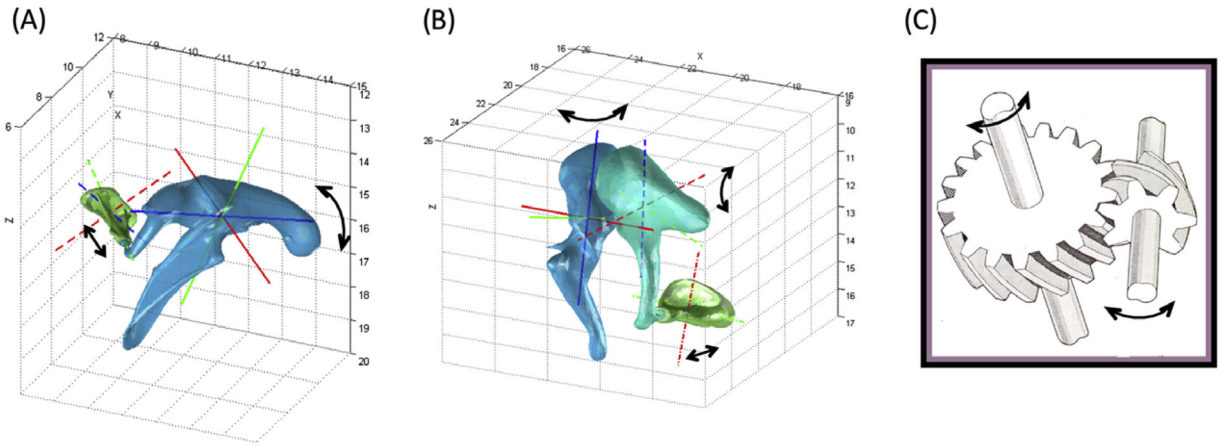

Fig. 6.

Summary of malleus–incus complex and stapes motions. (A) The classical “hinging” motion present at low frequencies for all four mammals and at high frequencies for those with a fused malleus–incus joint, as shown here for chinchilla. (B) A hypothesized high-frequency “twisting” motion of the malleus, which requires a 90° rotational axis shift to transfer motion to the incus and stapes, as shown here for human. (C) Crossed helical gears (shown) or bevel gears at right angles, commonly found in machinery, also provide a rotational axis shift (Nolk, 2000). In (A) and (B), blue lines indicate axes associated with the minimum moment of inertia (MOI), red lines with the maximum MOI, and green lines with the intermediate MOI.

Table 1

Cross-species comparison of the malleus–incus joint mobility, malleus + incus mass, minimum moment of inertia (Min MOI), and ratio of posterior and anterior eardrum areas (A_{post}/A_{ant}), with columns arranged in order of upper-frequency hearing limit for each species.

	Human	Chinchilla	Guinea pig	Cat
Malleus–incus joint mobility	Mobile	Fused[a]	Fused[b]	Mobile
Malleus + incus mass[c] (mg)	62	11	5	15
Min MOI (mg/mm^5)	6.8	4.3	1.2	2.2
A_{post}/A_{ant}	1.6	1.0	1.1	1.9
Upper-frequency hearing limit[d] (kHz)	20	23	49	64

[a] Vrettakos et al. (1988).

[b] Amin and Tucker (2006).

[c] Wever and Lawrence (1954), Nummela (1995).

[d] Fay (1988).